

RESEARCH ARTICLE

Open Access



# Hyaluronic acid/chitin thermosensitive hydrogel loaded with TGF- $\beta$ 1 promotes meniscus repair in rabbit meniscus full-thickness tear model

Ze Wang<sup>1†</sup>, Wei Huang<sup>2†</sup>, Shengyang Jin<sup>3†</sup>, Fei Gao<sup>2</sup>, Tingfang Sun<sup>2</sup>, Yu He<sup>2</sup>, Xulin Jiang<sup>4\*</sup> and Hong Wang<sup>2\*</sup>

## Abstract

Repair of the damaged meniscus is a scientific challenge owing to the poor self-healing potential of the white area of the meniscus. Tissue engineering provides a new method for the repair of meniscus injuries. In this study, we explored the superiority of 2% hyaluronic acid chitin hydrogel in temperature sensitivity, in vitro degradation, biocompatibility, cell adhesion, and other biological characteristics, and investigated the advantages of hyaluronic acid (HA) and Transforming Growth Factor  $\beta$ 1 (TGF- $\beta$ 1) in promoting cell proliferation and a matrix formation phenotype. The hydrogel loaded with HA and TGF- $\beta$ 1 promoted cell proliferation. The HA + TGF- $\beta$ 1 mixed group showed the highest glycosaminoglycan (GAG) content and promoted cell migration. Hydroxypropyl chitin (HPCH), HA, and TGF- $\beta$ 1 were combined to form a composite hydrogel with a concentration of 2% after physical cross-linking, and this was injected into a rabbit model of a meniscus full-thickness tear. After 12 weeks of implantation, the TGF- $\beta$ 1 + HA/HPCH composite hydrogel was significantly better than HPCH, HA/HPCH, TGF- $\beta$ 1 + HPCH, and the control group in promoting meniscus repair. In addition, the new meniscus tissue of the TGF- $\beta$ 1 + HA/HPCH composite hydrogel had a tissue structure and biochemical content similar to that of the normal meniscus tissue.

**Keywords** Hyaluronic acid, Hydroxypropyl chitin, TGF- $\beta$ 1, Thermosensitive hydrogel, Meniscus injury repair

<sup>†</sup>Ze Wang, Wei Huang and Shengyang Jin contributed equally to this work and share first authorship.

\*Correspondence:

Xulin Jiang  
xljiang@whu.edu.cn  
Hong Wang  
wanghwh@126.com

<sup>1</sup> Department of Orthopedics, Wuhan Children's Hospital (Wuhan Maternal and Child Healthcare Hospital), Tongji Medical College, Huazhong University of Science and Technology, Wuhan 430015, People's Republic of China

<sup>2</sup> Department of Orthopedics, Union Hospital, Tongji Medical College, Huazhong University of Science and Technology, Wuhan 430022, People's Republic of China

<sup>3</sup> Department of Orthopedics, The First Affiliated Hospital of Soochow University, Suzhou 215006, People's Republic of China

<sup>4</sup> Key Laboratory of Biomedical Polymers of Ministry of Education and Department of Chemistry, Wuhan University, Wuhan 430072, People's Republic of China



© The Author(s) 2024. **Open Access** This article is licensed under a Creative Commons Attribution-NonCommercial-NoDerivatives 4.0 International License, which permits any non-commercial use, sharing, distribution and reproduction in any medium or format, as long as you give appropriate credit to the original author(s) and the source, provide a link to the Creative Commons licence, and indicate if you modified the licensed material. You do not have permission under this licence to share adapted material derived from this article or parts of it. The images or other third party material in this article are included in the article's Creative Commons licence, unless indicated otherwise in a credit line to the material. If material is not included in the article's Creative Commons licence and your intended use is not permitted by statutory regulation or exceeds the permitted use, you will need to obtain permission directly from the copyright holder. To view a copy of this licence, visit <http://creativecommons.org/licenses/by-nc-nd/4.0/>.

## Introduction

The meniscus is a significant basic structure in the human knee joint. In the past, the meniscus was considered useless, but it is now recognized as an essential element in the stability, load, shock absorption, and lubrication of the knee joint. Meniscus repair can prevent the joint from increasing the load and can slow the progression of osteoarthritis [1, 2]. Research on the function of the meniscus and the development of arthroscopic technology has led to arthroscopic meniscus suture or molding becoming the standard treatment for meniscus injury repair [3]. However, it is difficult to repair the white area after the meniscus is sutured. Strengthening the activity and regeneration ability of the meniscus after repair and retaining the meniscus to the maximum are major challenges facing researchers [4].

Tissue engineering is attracting extensive attention as a promising method for meniscus repair. Appropriate tissue engineering materials can simulate the components of the meniscus, load growth factors or seed cells, induce the migration of meniscus regeneration-related cells, stimulate the growth and differentiation of cells in the meniscus injury, and promote regeneration of the damaged meniscus [5, 6]. Suitable tissue engineering materials should imitate the meniscus matrix in terms of structure and function and provide an environmental basis for the growth and differentiation of meniscus regeneration-related cells.

The ideal biological scaffold material should have excellent biological safety and cell adhesion, a suitable microstructure, and certain mechanical strength. The material should also be suitable for various injuries and arthroscopic minimally invasive environments [7, 8]. Considerable efforts have been made to identify suitable scaffolds and cell sources to simulate the natural meniscus. Mesenchymal stem cells are widely acknowledged as the preferred type of stem cell reported in various seed cells, especially bone marrow and synovium [5]. Chondrocytes and meniscal fibrochondrocytes (MFCs) might be reasonable candidates for meniscus tissue engineering because they can produce the major extracellular matrix (ECM) components of the meniscus [9, 10].

Biomaterials for meniscus tissue engineering can be divided into natural or synthetic components; examples include polyurethane [11], poly ( $\epsilon$ -caprolactone) [12], alginate [13], HA [14], collagen [15], silk fibroin [16], chitosan [17], and ECM [18]. These biomaterials aim to provide 3D support and scaffolding. However, composite materials usually exhibit better physicochemical and biological properties compared with single materials [19], and several composite scaffolds have been trialed for meniscus tissue regeneration [20–22].

Heat-sensitive, injectable, in-situ cross-linked hydrogel has attracted the attention of researchers. This hydrogel is a flowable liquid in a low temperature environment and gradually solidifies when injected into the body owing to the effect of body temperature. The advantages of injectable hydrogels are that they are administered in liquid form and can be loaded with biologically active substances. Meniscus repair requires a hydrogel system that can encourage the growth and proliferation of MFCs and strengthen the repair ability of meniscus damage. We selected 1, 2-propylene oxide to etherify chitin, and then added a propyl group after introducing a hydroxyl group. The modified hydroxypropyl chitin (HPCH) has good solubility, temperature sensitivity, and pH responsiveness [23]. HPCH can also be cross-linked by simply mixing after adding HA, which is abundant in the human body and is the main component of synovial fluid. HA can effectively protect the knee joint, delay the development of osteoarthritis, and regulate cell growth, proliferation, and differentiation [24, 25]. Various growth factors, such as transforming growth factor- $\beta$ 1 (TGF- $\beta$ 1), bone morphogenetic protein 2 (BMP-2), and Insulin-like growth factor 1 (IGF-1), can induce cell migration, promote cell proliferation, and secrete ECM [26–28]. Among these growth factors, TGF- $\beta$ 1 can effectively promote the growth of MFCs and the secretion of glycosaminoglycans, collagen fibers, and other major components that constitute the meniscus. Simultaneously, TGF- $\beta$ 1 also enhances the structural strength of the ECM, thereby promoting contact between the new meniscus tissue and normal tissues [29, 30].

In this study, we evaluated the biosafety, degradability, and adhesion of hydrogels, and investigated whether hydrogels loaded with HA and TGF- $\beta$ 1 could promote the migration and proliferation of MFCs and secrete ECM to enhance the healing potential of meniscus injuries. The study aimed to determine whether TGF- $\beta$ 1-incorporated HA/HPCH hydrogel is a good biological scaffold for meniscus tissue engineering.

## Materials and methods

### Preparation of composite hydrogel

HA/HPCH hydrogel was prepared with the mass ratio of 12:1 (HPCH:HA). Twenty milliliters of deionized water was added to 120 mg HPCH powder (pre-sterilized by ethylene oxide), magnetic stirred for 15 min until it was completely dissolved, and then placed at 4 °C. Next, 10 mg HA powder (2–4 million Da; Solarbio, Beijing, China) was added to the mixture, which was then placed in an ultrasonic cleaning machine and mixed for 15 min. This generated the HPCH/HA solution with a mass ratio of 12:1. The solution was stored at –20 °C overnight, and then freeze-dried for 24 h to obtain HPCH/HA powder.

TGF- $\beta$ 1 was supplied by MedChemExpress (NJ, USA). HPCH powder was supplied by Key Laboratory of Biomedical Polymers of Ministry of Education and Department of Chemistry, Wuhan University, Wuhan.

### Characterization of composite hydrogel

#### Scanning electron microscope (SEM)

HPCH hydrogel and HA/HPCH hydrogel were freeze-dried for 12 h. The resulting powder was carefully removed with a blade and applied to conductive glue on the objective table. The samples were then subjected to gold spraying treatment, and were examined by SEM (HITACHI Regulus 8100, 0.1–30 kV) and photographed.

#### Characterization of temperature sensitivity

The sol–gel transition temperature of the three groups of hydrogels (HPCH, HA/HPCH, and TGF- $\beta$ 1+HA/HPCH.) was measured by the bottle inversion method. The hydrogel is enclosed in a glass bottle, which is then immersed in a water bath for heating; 15 °C was used as the initial temperature and this was increased in 0.3 °C intervals [31]. Each group of glass bottles was removed after equilibrating for 5 min and the bottles were inverted 180° to observe the state of hydrogel. The temperature at which each group of hydrogels cannot fall back was recorded, and this is the sol–gel transition temperature of the sample.

#### Degradability of hydrogel

The weighing method was used to study the degradability of the three groups of hydrogels. Three groups of 2 wt% PBS-buffered hydrogel (GIBCO, USA) dispersions were prepared. Briefly, 2 mL of prepared hydrogel was placed in a mesh bag, which was wholly submerged into a centrifuge tube, and lysozyme (Sigma Aldrich, St Louis, MO, USA) solution was added to the centrifuge tube at a concentration of 500  $\mu$ g/ml. The centrifuge tube was incubated on a shaker (37 °C). The mesh bag was observed daily and the lysozyme solution was replaced daily. To weigh the hydrogel, the mesh bag was removed from the centrifuge tube and filter paper was used to absorb the water from the surface of the hydrogel. The dry weight of the hydrogel was recorded on day 0, 2, 4, 7, 14, 21, and 28, and the degradation rate on day  $t$  (%) =  $(m_0 - m_t) / m_0 \times 100\%$ , where the initial weight of each group of hydrogels is  $m_0$ , the weight of each group of hydrogels on day  $t$  is  $m_t$ , and each group has five parallel groups.

#### Isolation and cultivation of meniscus fibrochondrocytes (MFCs)

New Zealand white rabbits, age 3 months, were euthanized with pentobarbital (200 mg/kg). The meniscus of both knees of each rabbit were removed, the ligaments

and synovium attached to the meniscus were cleaned up, and the meniscus were dissected into 1 mm<sup>3</sup> pieces. The meniscus pieces were incubated with 0.25% trypsin in a shaking 37 °C water bath for 30 min. Next, 0.2% type II collagenase (GIBCO, USA) was added, and the samples were incubated in the 37 °C water bath with shaking for 4–6 h. The digestion was terminated when the tissue pieces were basically digested. The digestion solution was filtered through a 200-mesh screen and centrifuged at 1500 rpm for 10 min. The supernatant was discarded and then the precipitate was resuspended in complete DMEM (Sigma Aldrich, St Louis, MO, USA). The cells were resuspended in growth medium (10% fetal bovine serum (GIBCO, USA) in DMEM with 1% of penicillin and streptomycin) and incubated at 37 °C with an atmosphere of 5% CO<sub>2</sub> and 95% air.

#### Characterization of rabbit MFCs

The well-grown rabbit MFCs were subjected to cell-climbing, rinsed three times with PBS, fixed with 75% alcohol for 10 min, then rinsed twice with PBS, and stained with 1% toluidine blue solution for 10 min. The staining solution was aspirated, and the MFCs were rinsed three times with PBS and observed under an inverted phase-contrast microscope.

#### Biocompatibility of hydrogel

A cell counting kit 8 (CCK-8 kit; Solarbio, Beijing, China) was used to quantitatively evaluate the number of cells in the hydrogel with different mass volume fractions (0.1%, 0.5%, 2%, 4%), 100  $\mu$ l cell suspension ( $1 \times 10^5$ /ml) was added to a 96-well plate ( $n=5$ ). After incubation for 6 h, the culture medium was removed and different concentrations of HPCH, HA/HPCH, and TGF- $\beta$ 1+HA/HPCH complete medium hydrogel dispersions were added to the wells. The volume of each group was 100  $\mu$ l. The plates were incubated for 24 and 48 h, and cell-free hydrogel was added as a blank. PBS buffer solution has been used to wash the hydrogel on the ice before adding CCK-8. A microplate reader (Thermo Scientific (China) Co. Ltd.) was used to read the absorbance of the test solution ( $n=5$  per group) at 450 nm.

#### Cell adhesion of hydrogel

The Live-Dead Live Dead Cell Kit (Solarbio, Beijing, China) was used to detect five groups of hydrogels (HPCH, TGF- $\beta$ 1+HPCH, HA/HPCH, TGF- $\beta$ 1+HA/HPCH, control group) ( $n=5$ ). The materials of each group were prepared in 2% PBS-buffered hydrogel, and 300  $\mu$ L of hydrogel was added to a 48-well plate and incubated at 37 °C for 30 min. Next, 300  $\mu$ L rabbit MFCs ( $2 \times 10^5$ /ml) was added to each well and the plates were incubated in a CO<sub>2</sub> incubator at 37 °C for 4 h, then were

incubated in a PBS solution containing 2 mM calcein AM and 4 mM ethidium homodimer1 at 37 °C for 40 min. The number and morphology of the cells was observed under an inverted fluorescence microscope (Primovert, Carl Zeiss, Germany), taking pictures and calculating the number of cells in each group. The images were analyzed by ImageJ software, and the cell adhesion rate was calculated as:

Cell adhesion rate (%) =  $Q_t/Q_c \times 100\%$ . Where  $Q_t$  is the experimental group, and  $Q_c$  is the control group.

### Characterization of three-dimensional cell culture

#### Cell proliferation assay

CCK-8 was used to quantitatively determine the proliferation of three groups of hydrogels (HPCH, HA/HPCH, and TGF- $\beta$ 1 + HA/HPCH) ( $n=5$ ) at 0, 24, and 48 h. Briefly, 100  $\mu$ l hydrogel-cell mixture with a mass volume fraction of 2% was added to a 96-well plate, and incubated for 24 or 48 h at 37 °C with and atmosphere of 5% CO<sub>2</sub> and 95% air. A microplate reader (Thermo Scientific (China) Co. Ltd. China) was used to read the absorbance of the test solution ( $n=5$  for each group) at 450 nm.

#### SEM

The HPCH, HA/HPCH, and TGF- $\beta$ 1 + HA/HPCH hydrogel-cell mixtures were cultured for 48 h, quick-frozen with liquid nitrogen, and placed in a pre-cooled vacuum freeze dryer for 24 h. After sample preparation and gold spray treatment, SEM was used to observe the morphological characteristics of the cells in the hydrogel.

#### Biochemical assays for glycosaminoglycan (GAG)

A rabbit GAG ELISA kit (Keshun Science and Technology Co. Shanghai, China) was used to quantitatively detect the amount of GAG secreted by cells. 0.5 mg/ml HA, 1 mg/ml HA, 1 ng/ml TGF- $\beta$ 1 and 10 ng/ml TGF- $\beta$ 1 were added to the cell culture medium, respectively. 0.5 mg/ml HA and 1 ng/ml TGF- $\beta$ 1 were added in group five, and 1 mg/ml HA and 1 ng/ml TGF- $\beta$ 1 were added in group six. A total of 0.5 ml of cell suspension ( $5 \times 10^5$ /ml) was added to each well of a 6-well plate. The culture medium was changed and collected every 3 days. The manufacturer's instructions were followed to add reagents of the rabbit GAG ELISA kit and detect GAG.

#### Cell migration experiment

The scratch test was used to determine the effects of HA and TGF- $\beta$ 1 on cell migration. A 0.5 mm  $\times$  0.5 mm criss-cross grid was drawn on a white paper, and the cell culture dish full of cells was placed on it. Cells in the culture dish were scratched along horizontal and vertical lines with a 200  $\mu$ l sterile pipette tip, changing the medium to remove the exfoliated cells. To ensure the consistency of

the degree of cell damage, the scratching operation was performed by a dedicated person, and each dish had the same number of horizontal and vertical lines.

### In vivo implantation

#### Surgical procedure

A total of 45 New Zealand white rabbits were randomly divided into 5 groups ( $n=9$ ) to create a meniscus full-thickness injury model as follows: control group, HPCH group, HA/HPCH group, TGF- $\beta$ 1 + HA/HPCH group, and TGF- $\beta$ 1 + HPCH group (the final concentration of TGF- $\beta$ 1 is 100 ng/mL). After anesthetizing the rabbits, a sharp blade was used to make a longitudinal full-thickness tear of approximately 5 mm along the white area of the medial meniscus to the anterior corner, and then the meniscus was carefully reset. The experimental group was injected with approximately 0.3 ml low-temperature liquid hydrogel, which was heated to turn it into a gel state, and the incision was fixed by the tension of the hydrogel. The joint capsule, subcutaneous tissue, and skin were sutured layer by layer, and penicillin was injected intramuscularly after the operation at 10,000 U/kg. The inner side of the knee joint was fixed with a self-made small splint. Penicillin was injected intramuscularly at 30,000 U/kg every day for 3 days after the operation. At 4, 8, and 12 weeks after the operation, three rabbits were randomly selected from each group for assessment after being euthanized.

#### Morphological observations

The injured menisci were observed and photographed, observing the activity of the rabbit, joint cavity effusion, adhesion, synovial hyperplasia, meniscus repair, whether the meniscus is flat, whether the incision is healed, the texture and luster of the meniscus and the femur, whether the condyle cartilage is damaged or degenerated, whether the material remains, and whether there is adhesion in the joint cavity.

#### Histological analysis

Menisci were fixed in 4% paraformaldehyde for 48 h, embedded in paraffin, cut into 7- $\mu$ m sections, and stained with hematoxylin and eosin (H&E), toluidine blue, and safranin-O-fast green.

#### Statistical analysis

SPSS 24.0 software was used for statistics and analysis of all data, and paired sample  $t$ -tests were used;  $P \leq 0.05$  indicates that the difference is statistically significant. GraphPad Prism 8 software was used to draw graphs, and all experiments were repeated three times.

## Results

### Characterization of HPCH-based hydrogels

The SEM images of the hydrogels (Fig. 1) show that each group of hydrogels has a loose and porous structure, and the pores are connected to each other, which is conducive to the circulation of various substances between the materials. The pore walls of the hydrogel can load HA and growth factors. Compared with HPCH with HA, pure HPCH has a more orderly structure and smooth pore walls. The addition of HA leads to more branches in the pore-wall structure, which may increase the hydrophilicity of the material and reduce structural strength of the material. The proportion of HA added in this experiment is relatively low, which has a weak effect on the structure of the material and maintains the structural strength of pure HPCH. Therefore, both the pure HPCH and the HPCH material with HA could meet the structural requirements of the scaffold material, and subsequent cell and animal experiments could be performed.

### Analysis of temperature sensitivity of hydrogel

The transition temperature of HPCH PBS buffer hydrogel (2 wt%) is 21.18 °C, that of the HA/HPCH PBS buffer hydrogel sol-gel is 21.48 °C, and that of HA + TGF- $\beta$ 1/HPCH PBS buffer hydrogel sol-gel is 21.48 °C (Fig. 2). With the increase of temperature, the gel undergoes multiple coil-to-globule transitions. This hydrophilicity-hydrophobicity transformation was due to the formation of multiple interchain/intrachain hydrogen bonds [32]. The sol-gel transition temperature of the hydrogel increased slightly after adding HA, which may be due to the hydrophilicity of HA and the formation of hydrogen bonds between chitin [33]. The hydrogel network after adding HA has more hydrogen bonds. High temperature

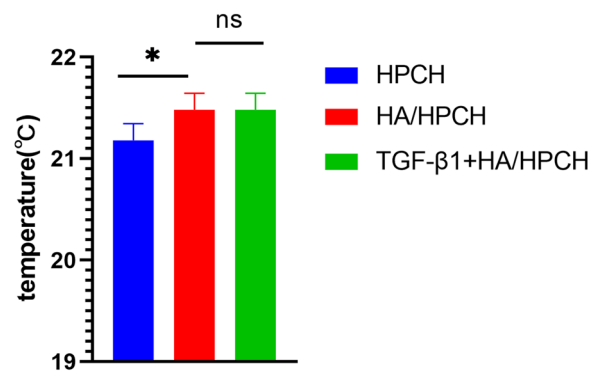


**Fig. 2** Sol-gel transition temperature of HPCH, HA/HPCH, and TGF- $\beta$ 1 + HA/HPCH PBS buffer solutions with a mass volume fraction of 2 wt%. (\* $P < 0.05$ , ns  $P > 0.05$ )

breaks the hydrogen bonds and completes the transformation of hydrogelation. However, because the content of HA in the material is low, the temperature rise is not obvious. The sol-gel transition temperature of the hydrogel after adding TGF- $\beta$ 1 did not change compared with the hydrogel without TGF- $\beta$ 1.

### Degradability analysis of hydrogel

Figure 3 shows that when the lysozyme concentration was 500  $\mu$ g/l and the temperature was 37 °C, the hydrogels of each group were degraded within 4 weeks and only approximately 8% remained. Moreover, the degradation rate of each group of hydrogels was essentially the same. The degradation rate of the general polymer is lower when the molecular weight is larger, but HA was not hydrolyzed by lysozyme [34]. HA in the mixture did not affect the degradation rate. Furthermore, as the amount of growth factor TGF- $\beta$ 1 added to the mixture is

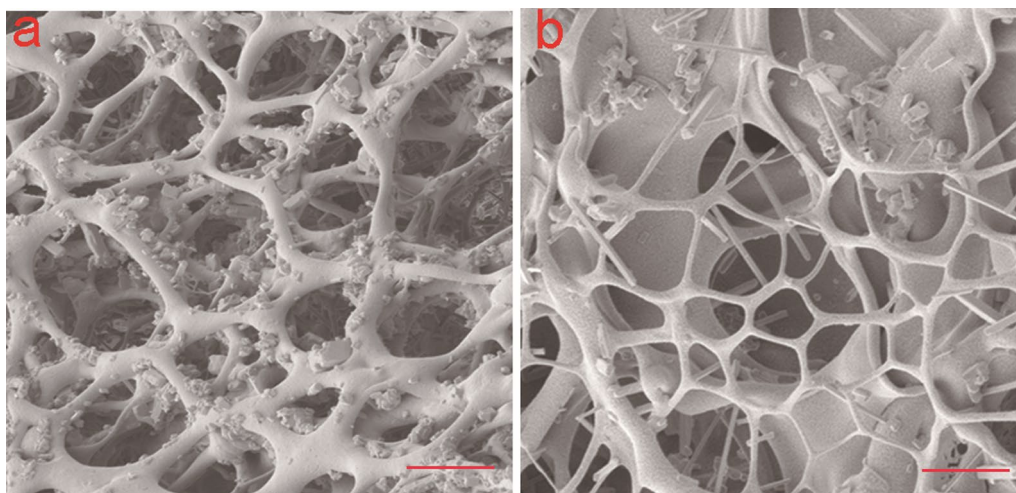


**Fig. 1** Electron microscopic ultrastructure of hydrogel. **a** HA/HPCH; **b** HPCH. Scale bar, 100  $\mu$ m

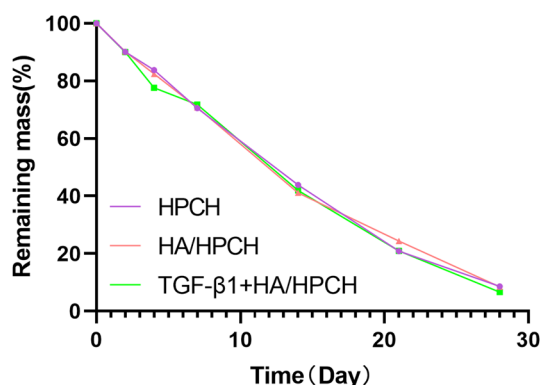


**Fig. 3** Degradation of HPCH, HA/HPCH, TGF-β1 + HA/HPCH with a mass volume fraction of 2 wt% at 37 °C and a lysozyme concentration of 500 μg/ml

very small and will not affect the degradation rate of the hydrogel, the degradation rate of each group of hydrogels is almost identical, indicating that the material has good degradability *in vitro*. Human synovial fluid is rich in lysozyme [35], so the hydrogel will be degradable in the human body.

#### Characterization of rabbit MFCs

The primary MFCs extracted by the initial digestion were transparent and small spherical-shaped. After 12–24 h, the cells began to adhere to the wall, and gradually deformed and stretched into a polygonal and spindle shape. After approximately 10 days of culture, the cells cover the bottom of the bottle, showing a typical paving stone-like appearance (Fig. 4). The bottom of the bottle can be covered in cells after 7 days of culture. The cytoplasm of the cultured MFCs and the surrounding secretions were blue following toluidine blue staining (Fig. 4c). This is because the cytoplasm and the secretions around the cells contain GAG, and this produces a blue reaction with toluidine blue, which is characteristic of fibrochondrocytes.

#### Cell survival rate analysis

HPCH, HA/HPCH, and TGF-β1 + HA/HPCH hydrogels with different mass and volume fractions were incubated with MFCs for 24 h and cell survival was determined. The average survival rate of MFCs was greater than 95% for each group of hydrogels (HPCH, HA/HPCH, and TGF-β1 + HA/HPCH) with mass volume fractions of 0.1%, 0.5%, 2%, and 4% (Fig. 5a). The high survival rate of the cells in each group of hydrogels after 24 h of culture indicates that the biological safety of the materials is good.

After 48 h of co-incubation, the average survival rate of HPCH hydrogel MFCs in each group with a mass volume fraction of 0.1%, 0.5%, and 2% was greater than 95%, and that for the MFCs in HPCH hydrogel with a mass volume fraction of 4% was 88% (Fig. 5b). The average survival rate of the HA/HPCH group with a mass volume fraction of 0.1%, 0.5%, and 2% is also greater than 100%, and the average survival rate of MFCs in the HA/HPCH hydrogel with a mass volume fraction of 4% is less than that of the first three groups. The average survival rate of the TGF-β1 + HA/HPCH group with a mass volume fraction of 0.1%, 0.5%, and 2% was also greater than 100%, while that of the TGF-β1 + HA/HPCH hydrogel with a mass volume fraction of 4% was lower compared with the first three groups.

Four kinds of composite hydrogels with different mass and volume fractions have no obvious cytotoxicity to MFCs, and the material has good biological safety. When the mass volume fraction reached 4%, the average survival rate was unchanged after 24 h of culture, but began to decrease after 48 h of culture. This may be because the pore structure becomes smaller, which affects the exchange of substances between the cells and the outside medium and air. When the number of cells is low in the early stage, cell growth is unaffected, but as the culture time increases, the number of cells will increase and cell growth is affected.

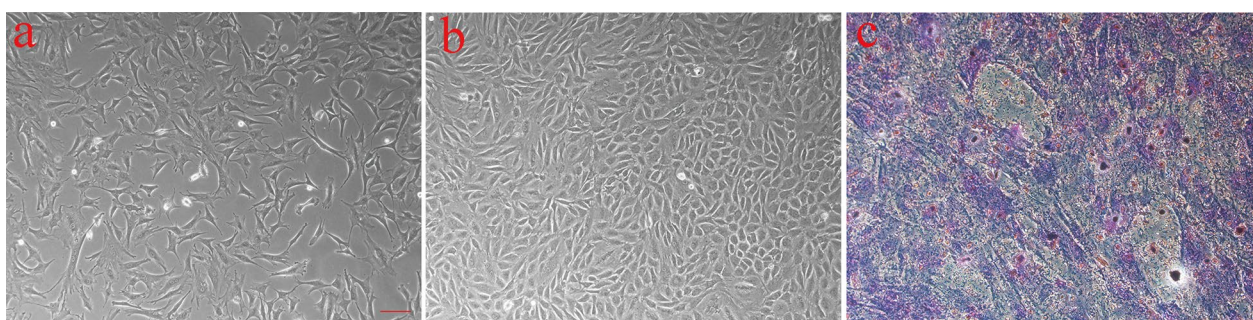


**Fig. 4** MFCs under the microscope. **a** MFCs began to deform; **b** MFCs covered the bottom of the bottle, forming a paving stone-like appearance; **c** MFCs toluidine blue staining. Scale bar, 100 μm

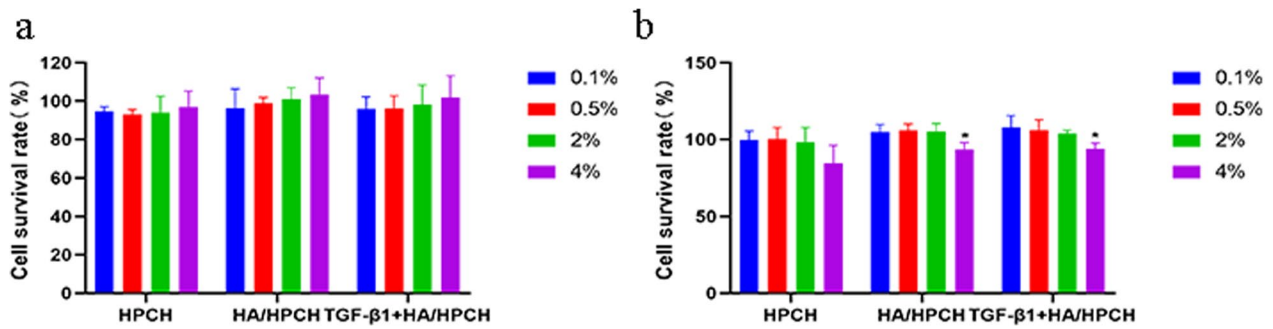
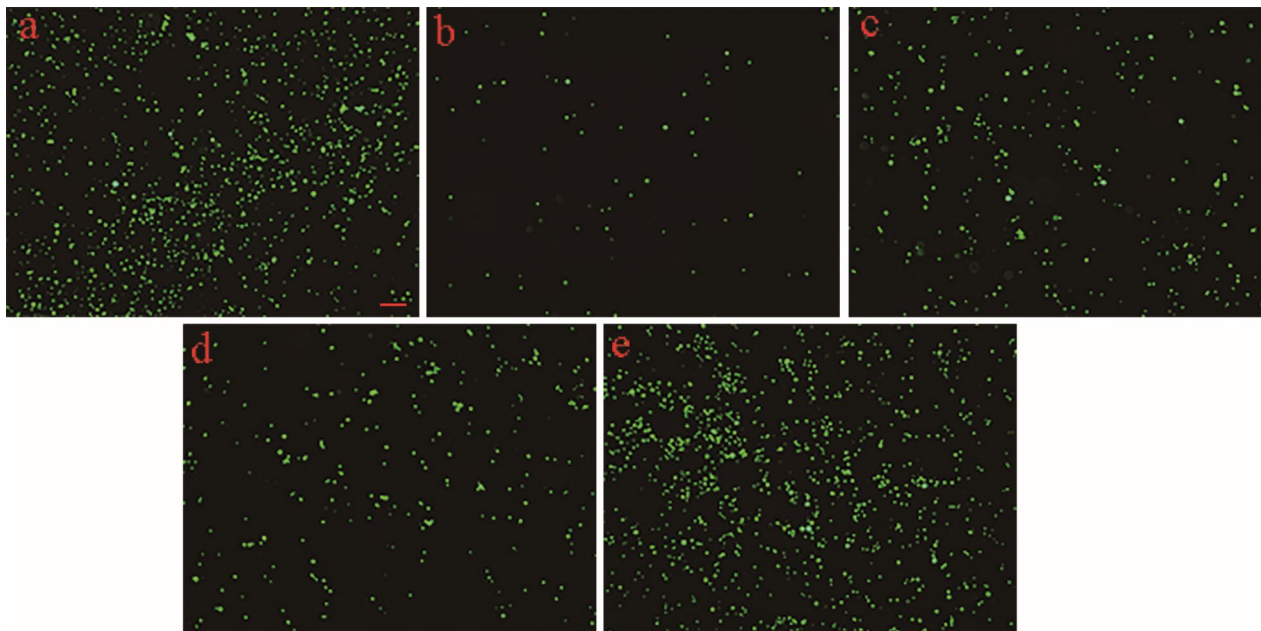


**Fig. 5** a Cell survival rates of HPCH, HA/HPCH, and TGF-β1 + HA/HPCH hydrogels with different mass and volume fractions and MFCs incubated for 24 h; b Cell survival rates of HPCH, HA/HPCH, and TGF-β1 + HA/HPCH hydrogels with different mass and volume fractions and MFCs incubated for 48 h. (\* $P < 0.05$ )

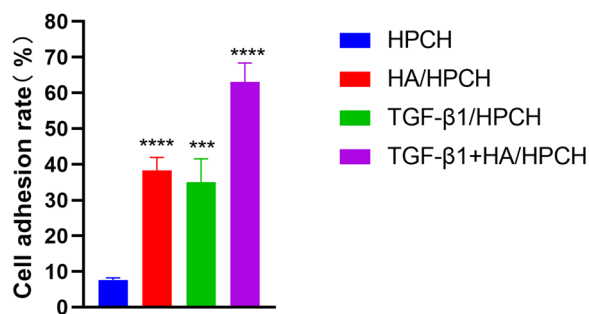
### Cell adhesion analysis

Figure 6 shows each group of a–e is full of green fluorescence and almost no red fluorescence, indicating that there are no dead cells and no obvious biological toxicity of each group of hydrogels. This is consistent with the result obtained in 2.4.2. Compared with group a, the number of cells in group b was significantly reduced, indicating that the adhesion of pure HPCH hydrogel cells was poor; the number of cells in group c was more than that in group b, but still less than that in group a, indicating that the addition of HA increased the adhesion of the material to the MFCs. The number of cells in group d is higher than that in group b, but still less than that in

group a, indicating that the addition of TGF-β1 increases the adhesion of the material to MFCs. Compared with group c, the number of cells in group d was not significantly different, implying that the adhesion of TGF-β1 to MFCs was not significantly different to that of HA. The number of cells in group e was greater than that in group b and was very similar to the number of cells in group a, indicating that the addition of HA and TGF-β1 significantly increased the adhesion of the material to MFCs. Calculating the cell adhesion of each group (Fig. 7) shows that the adhesion rate of HPCH to MFCs is 7.6%, and there is almost no adhesion. Both HA and TGF-β1 can increase the adhesion of materials to MFCs, The adhesion



**Fig. 6** Cell adhesion following incubation for 4 h with: a untreated cells; b HPCH; c HA/HPCH; d TGF-β1/HPCH; e TGF-β1 + HA/HPCH. Live (green) and dead (red) cells were stained in each group. Scale bar, 100 μm



**Fig. 7** Cell adhesion rate of each group of hydrogels. (\*\*\* $P < 0.001$ , \*\*\*\* $P < 0.0001$ )

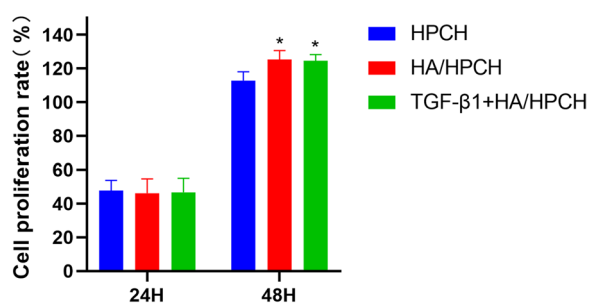


**Fig. 8** Cell proliferation rate of each group of hydrogels at 24 and 48 h. (\* $P < 0.05$ )

rate in the HA/HPCH group was 38.3%, and the adhesion rate in the TGF-β1/HPCH group was 35.1%. However, there was no statistical difference in the increase in adhesion to MFCs between the two. The adhesion rate of the composite TGF-β1 + HA/HPCH hydrogel to MFCs was 66.9%.

#### Cell proliferation in three-dimensional culture

After 24 h in three-dimensional culture, the cell proliferation rate of the three groups (HPCH, HA/HPCH, and TGF-β1 + HA/HPCH) was approximately 43%, and

there was no significant difference in cell proliferation among the groups (Fig. 8). After 48 h of incubation, the average cell growth of the HPCH group exceeded 110%, while that of the HA/HPCH group and the TGF-β1 + HA/HPCH group exceeded 120%. This indicated that the three groups of cells increased significantly. The growth rate of cells in the HA/HPCH group and the TGF-β1 + HA/HPCH group were relatively similar and greater than the HPCH group and the difference was statistically significant ( $P < 0.05$ ), while there was no significant difference in the cell proliferation rate between the HA/HPCH group and the TGF-β1 + HA/HPCH group. This shows that the cells can not adapted to the culture environment at the initial stage of the co-cubation, and their growth retarded. As the culture time increases, after the cell culture conditions are stabilized, the growth rate increases. After adding HA, the cell proliferation rate gradually increased, indicating that HA can promote the proliferation of MFCs. The three groups of cells all proliferate significantly, indicating that the hydrogel material will not cause damage to MFCs and the cells can proliferate normally.

#### Characterization of three-dimensional cell culture

Figure 9 is a SEM image of each group of hydrogels with freeze-dried powder of MFCs after 48 h of culture. Compared with the hydrogels that were not co-cultured with cells, there are more spherical cell structures on the pore walls and more spherical cell structures around the cells. The many silk-foot-like structures, which are a polygonal structure of deformed MFCs, indicates that MFCs can grow on the pore walls of the hydrogel. The loose and porous structure also facilitates the exchange of substances between cells and the outside world. Simultaneously, there is enough space in the pores for cell growth and proliferation.

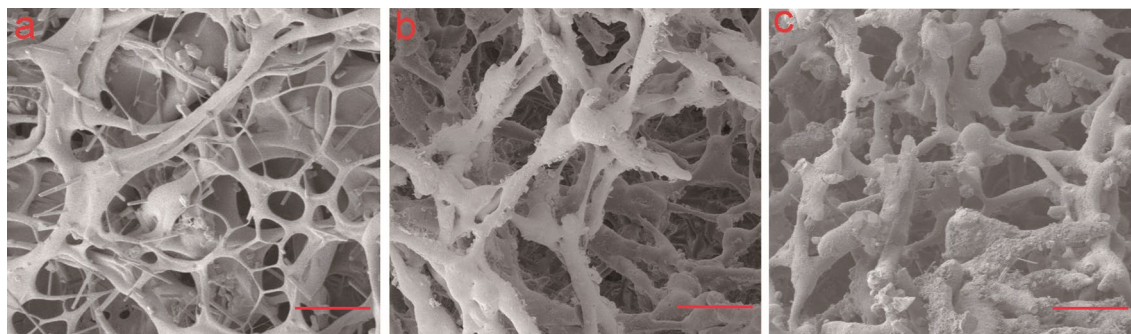


**Fig. 9** SEM image of MFCs and the hydrogels HPCH (a), HA/HPCH (b), and TGF-β1 + HA/HPCH (c) after 48 h lyophilized three-dimensional culture. Scale bar, 100 μm

### Biochemical assays for GAG

The added components in the composite material are crucial to the biological effects of cells. Figure 10 shows the results of GAG secretion by MFCs. Low concentrations of HA have no significant effect on the secretion of GAG by MFCs, while high concentrations of HA can significantly promote GAG secretion. Compared with the high concentration of HA, the low concentration of TGF- $\beta$ 1 has a slightly stronger effect on promoting the secretion of GAG, and the high concentration of TGF- $\beta$ 1 further enhances the secretion of GAG. Moreover, application of HA and TGF- $\beta$ 1 together promotes more GAG secretion than the single components. The largest amount of GAG secretion was obtained after treatment with high concentrations of HA and TGF- $\beta$ 1, indicating that HA and TGF- $\beta$ 1 in the composite material can promote the secretion of GAG from MFCs. GAG is the main component of the extracellular matrix of the meniscus, the HA and TGF- $\beta$ 1 in the composite material can enhance the secretion of the ECM of MFCs and enhance its repair potential.

### Scratch test analysis

After the cells were cultured for 24 h following the scratch experiment, the scratches in the control group were 428  $\mu$ m (Fig. 11). After adding HA and TGF- $\beta$ 1 separately, the scratch size was smaller. The effect of high-concentration HA was more obvious than that of low-concentration HA. The scratch size is minimal when HA and TGF- $\beta$ 1 were added, and the promotion effect of HA and TGF- $\beta$ 1 can be superimposed on each other. Therefore, HA and TGF- $\beta$ 1 in the composite material can promote the migration of MFCs and strengthen their repair potential.

### In vivo animal study

#### Macroscopic evaluation

All rabbits moved freely, and the rabbits in the experimental group had no complications such as joint infection, joint cavity effusion, or joint stiffness. The hydrogel material has been completely decomposed, and there was no residue or obvious inflammation (Fig. 12). The TGF- $\beta$ 1+HA/HPCH group has the strongest repair effect on the meniscus; the HA/HPCH group and the TGF- $\beta$ 1+HPCH group have a slightly weaker repair effect; and the HPCH group has no repair effect but can slightly protect the knee joint, possibly by the injection of hydrogel reducing the friction of the meniscus injury on the joint cavity. After the hydrogel is degraded, the joint degeneration begins; the meniscus injury in the control group is not repaired at all, and as time goes on, the acute meniscus injury develops into chronic meniscus injury and the joint degeneration gradually worsens. At 4 weeks post-operation, the meniscus new tissue in each group could not completely repair the defect. However, 8 weeks after the operation, the meniscus was almost completely repaired in the TGF- $\beta$ 1+HA/HPCH group with more new tissue. The meniscus surfaces of the HA/HPCH group and the TGF- $\beta$ 1+HPCH group also still have rough depressions. While that of the TGF- $\beta$ 1+HA/HPCH group is smooth and has been completely repaired in general observation at 12 weeks. The meniscus surfaces of the HA/HPCH group and the TGF- $\beta$ 1+HPCH group also still have rough depressions. This shows that TGF- $\beta$ 1+HA/HPCH hydrogel has a good meniscus repair effect.

#### Histological observations

In the TGF- $\beta$ 1+HA/HPCH group, a large number of elongated fibroblast-like cells or round chondrocyte-like cells were observed following H&E staining, and the collagen fibers in the repaired tissue gradually became regular (Fig. 13). With toluidine blue and safranin-O-fast

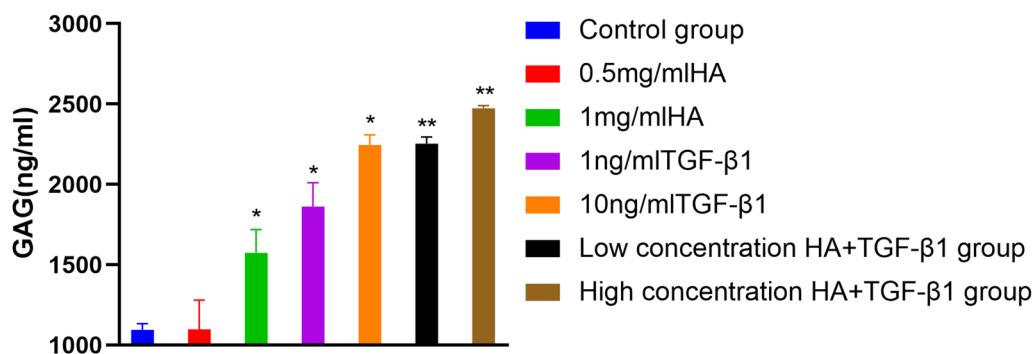


**Fig. 10** GAG content secreted by cells in each group. (\* $P$ <0.05, and \*\* $P$ <0.01)

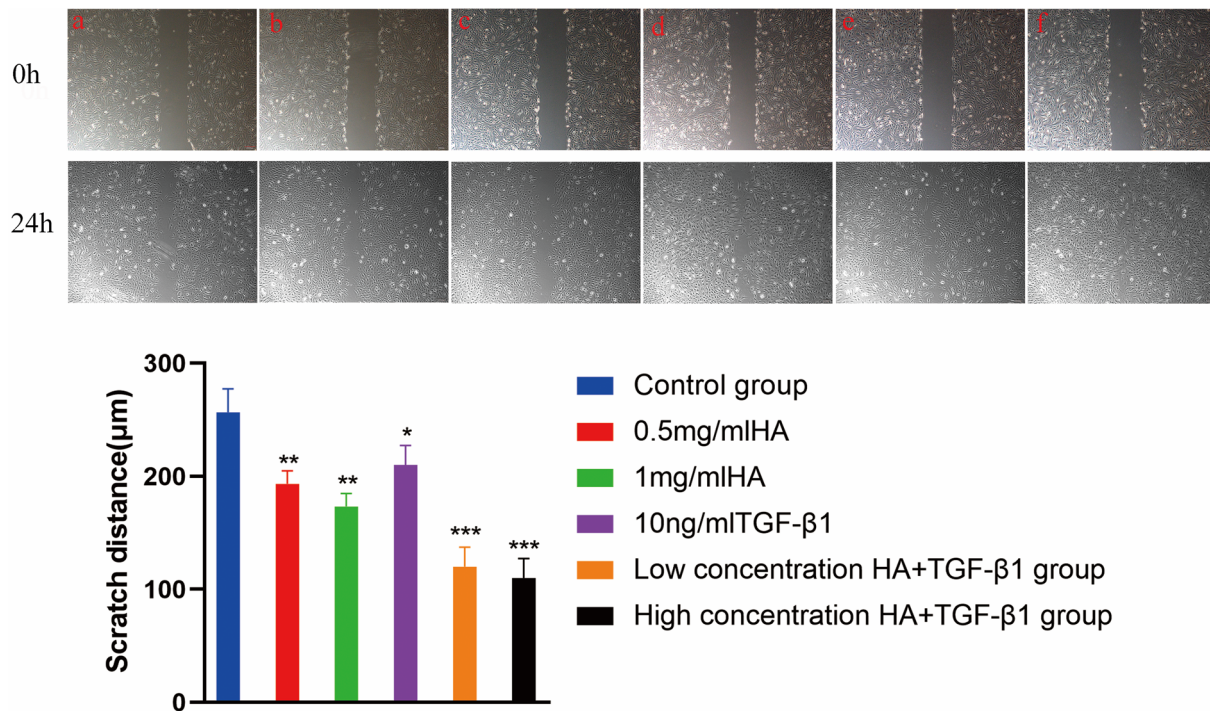


**Fig. 11** Scratch test image. **a** Control group; **b** 0.5 mg/mL HA; **c** 1 mg/ml HA; **d** 10 ng/ml TGF-β1; **e** low concentration HA+TGF-β1; **f** high concentration HA+TGF-β1. Magnification, Scale bar, 100 μm

green staining, numerous aggregated glycosaminoglycans were visible. In the HA/HPCH group, TGF-β1+HPCH group, and TGF-β1+HA/HPCH group, there were fibroblast-like cells or round chondrocyte-like cells in the repair area in the H&E staining. Glycosaminoglycan aggregation can be seen in toluidine blue and safranin-O-fast green staining (Figs. 14 and 15).

TGF-β1+HA/HPCH hydrogel effectively repaired the damaged meniscus; the meniscus was completely repaired after 12 weeks, and there was no obvious difference between new tissue and normal tissue. TGF-β1+HPCH and HA/HPCH hydrogels demonstrated obvious repairing effects on the meniscus, which was almost completely repaired after 12 weeks; the meniscus surface is slightly sunken and the internal collagen fibers

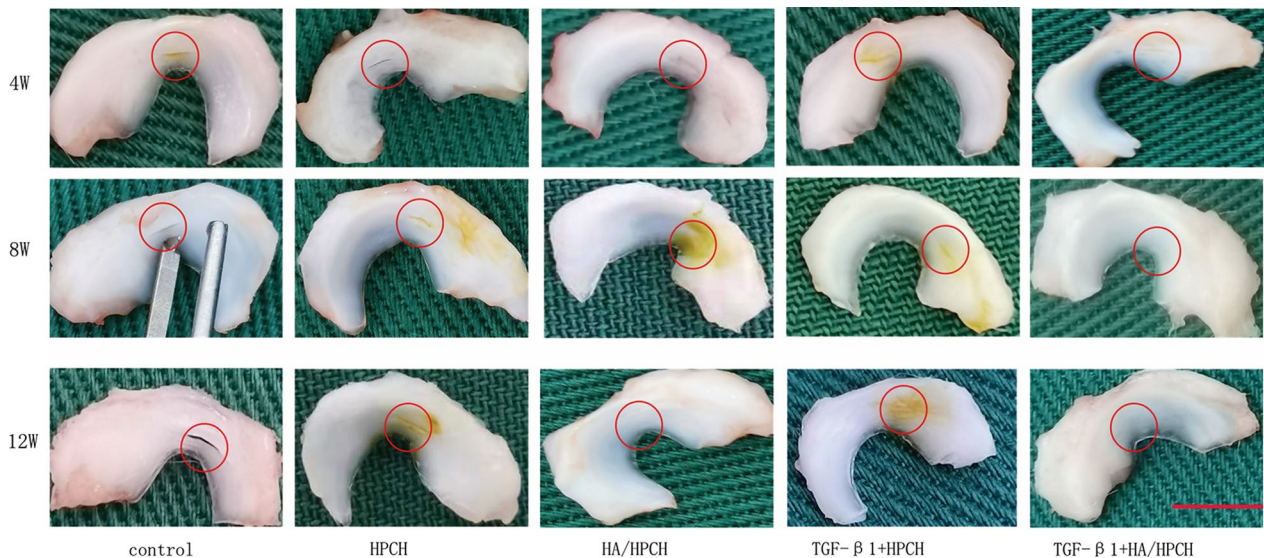


**Fig. 12** Representative images of menisci at 4, 8, and 12 weeks post-operation. Scale bar, 1 cm

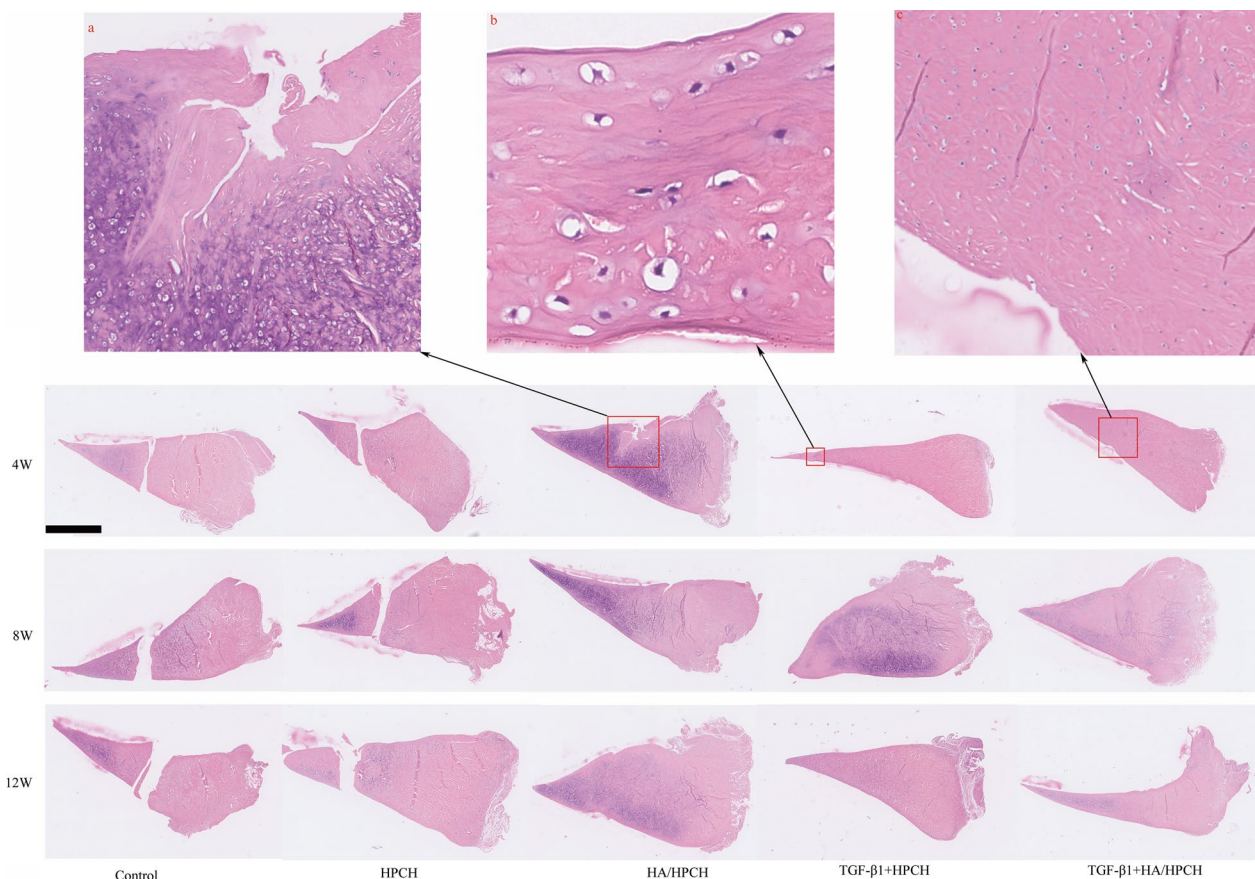


**Fig. 13** H&E staining of menisci. Group A, HA/HPCH; group B, TGF- $\beta$ 1 + HPCH; group C, TGF- $\beta$ 1 + HA/HPCH. Scale bar, 1 mm

are slightly disordered. In contrast, the menisci of the control group and the HPCH group did not heal at all. This indicated that the HPCH hydrogel has no repairing effect on the meniscus and only provides a stent effect.

## Discussion

Meniscus injury is a common disease in the clinic. According to the anatomy and internal blood supply, the meniscus is divided into red zone, red and white zone, and white zone. The red area is rich in blood vessels and has repair potential after injury, while the white area lacks a blood supply. Nutrition predominantly comes from the synovial fluid and the meniscus cannot repaired by itself after injury [1]. In this study, the menisci of the rabbits in the control group did not heal during the whole experiment, which is consistent with the phenomenon that the white area cannot be repaired after injury. In recent years, tissue engineering materials have attracted considerable attention for meniscus injury repair, and research on scaffold materials, seed cells, and growth factors is gradually increasing [36]. The purpose of this study was to explore the

effect of HA/HPCH scaffold material loaded with TGF- $\beta$ 1 to treat rabbit meniscus injury. In the rabbit meniscus longitudinal tear model, it was verified that TGF- $\beta$ 1 combined with HA/HPCH scaffold material can effectively promote the repair of meniscus injury. This provides a new idea for the treatment of meniscus injuries in the clinic.

We selected growth factors and concentrations based on previous literature on meniscus cells [37]. When 10 or 100 ng/ml TGF- $\beta$ 1 was added, proliferation increased, but no differences were observed between 10 and 100 ng [38]. TGF- $\beta$ 1 significantly increased the formation of GAGs [39]. Considering that the presence of synovial fluid in the articular cavity will lead to a decrease in the concentration of growth factor, we selected the concentration of 100 ng/ml.

At low temperatures, thermosensitive hydrogel remains liquid, which can be better mixed with other materials. There is no need for a complicated cross-linking process, it only needs to be stirred and mixed. Chitin contains a large number of amino groups, and HA contains numerous carboxyl groups, which may be bound by hydrogen

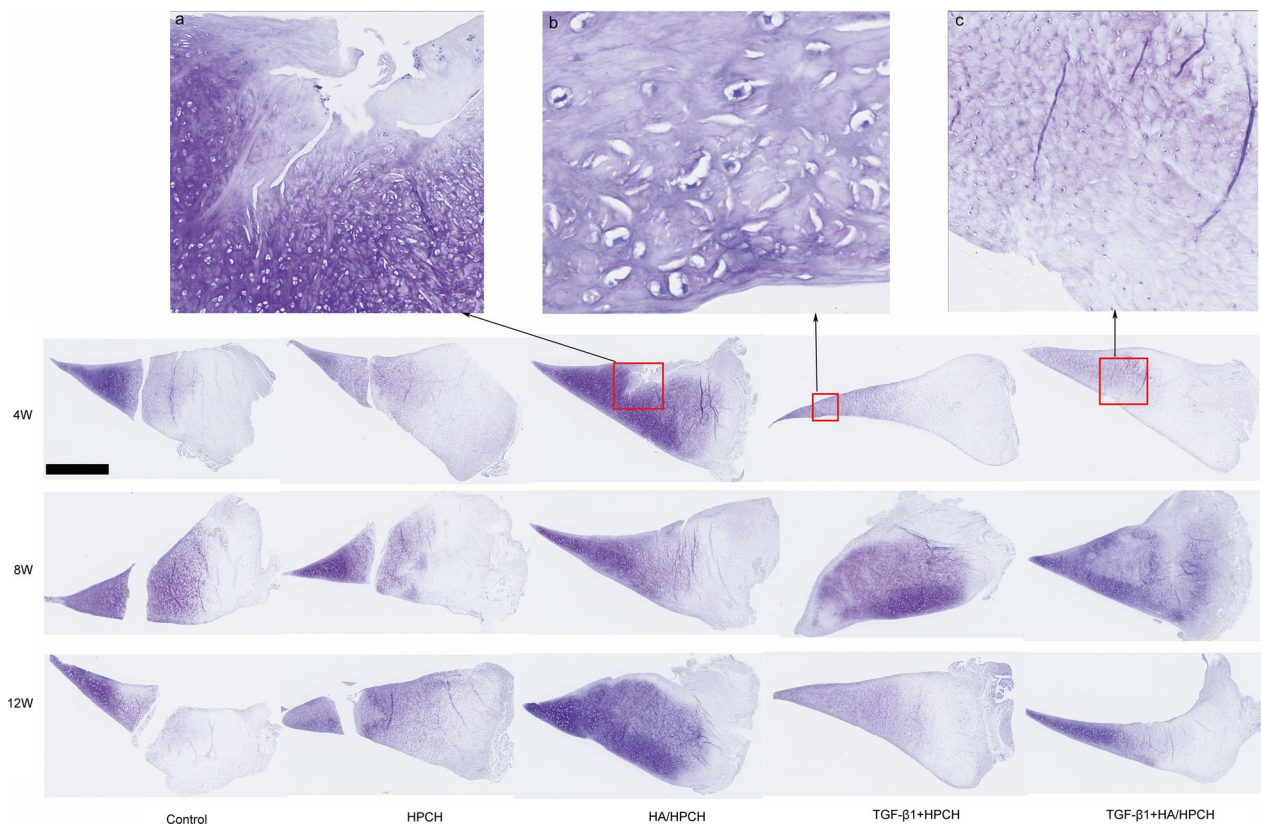


**Fig. 14** Toluidine blue staining of menisci. Group A, HA/HPCH; group B, TGF- $\beta$ 1 + HPCH; group C, TGF- $\beta$ 1 + HA/HPCH. Scale bar, 1 mm

bonds [33]. When the hydrogel material is in a liquid state, it can be directly injected into the area to be repaired, and there is no need for a large surgical area [40]. The hydrogel itself has a loose and porous structure, which is conducive to the attachment of cells. It can also be used as a load material for growth factors or drugs to prolong the action time of growth factors or drugs in the body [41]. A recent study found that HA enhances meniscus cell migration, promotes cell migration, and inhibits apoptosis [42]. Chitin plays an important role in tissue engineering. The product of chitin deacetylation is chitosan. HA and chitosan blends are increasingly studied [33]. Nano-scale delivery systems based on HA and chitosan are promising therapeutic tools in the local treatment of chronic wounds [43]. Tan synthesized *N*-succinyl-chitosan and aldehyde HA for preparation of the composite hydrogels, and this supported chondrocyte adhesion and encapsulation [44].

Before then, several investigators have attempted to use scaffolds to repair meniscus. 3D porous PU scaffolds by hMSCs highlights its efficacy in cartilage tissue regeneration, there is not a fully functional meniscus construct [11]. Li et al. developed a meticulously tailored PCL/SF scaffold augmented by SMSC affinity peptide L7 using

3DP technology, which has excellent structural, biomechanical, and functional properties for meniscus regeneration [22]. Our thermosensitive hydrogel comes from a wide range of sources and can be cross-linked in-situ, which can overcome the limitations of the traditional crosslinking method.

The thermosensitive hydrogel converts to a gel state after heating up, which can provide a certain strength of compressive capacity and a partial cushioning effect to protect the defective part. TGF- $\beta$ 1 + HA/HPCH hydrogel exhibited good healing effects of meniscal defects at 4–12 weeks. Cartilage lacuna and GAG were present in the repaired tissue, indicating that the repaired tissue is not only fiber healing, but is manifested as fibrocartilage-like healing, and MFCs were present and ECM was secreted. The gross and histological results demonstrated that there was no obvious inflammatory reaction in the rabbit knee joint after surgery. These findings indicate that the injection of TGF- $\beta$ 1 + HA/HPCH hydrogel significantly enhances the repair of the rabbit meniscus after full-thickness injury, and there are no obvious side effects.

In addition, there was no meniscus repair response in the control group and HPCH group, and an inflammatory

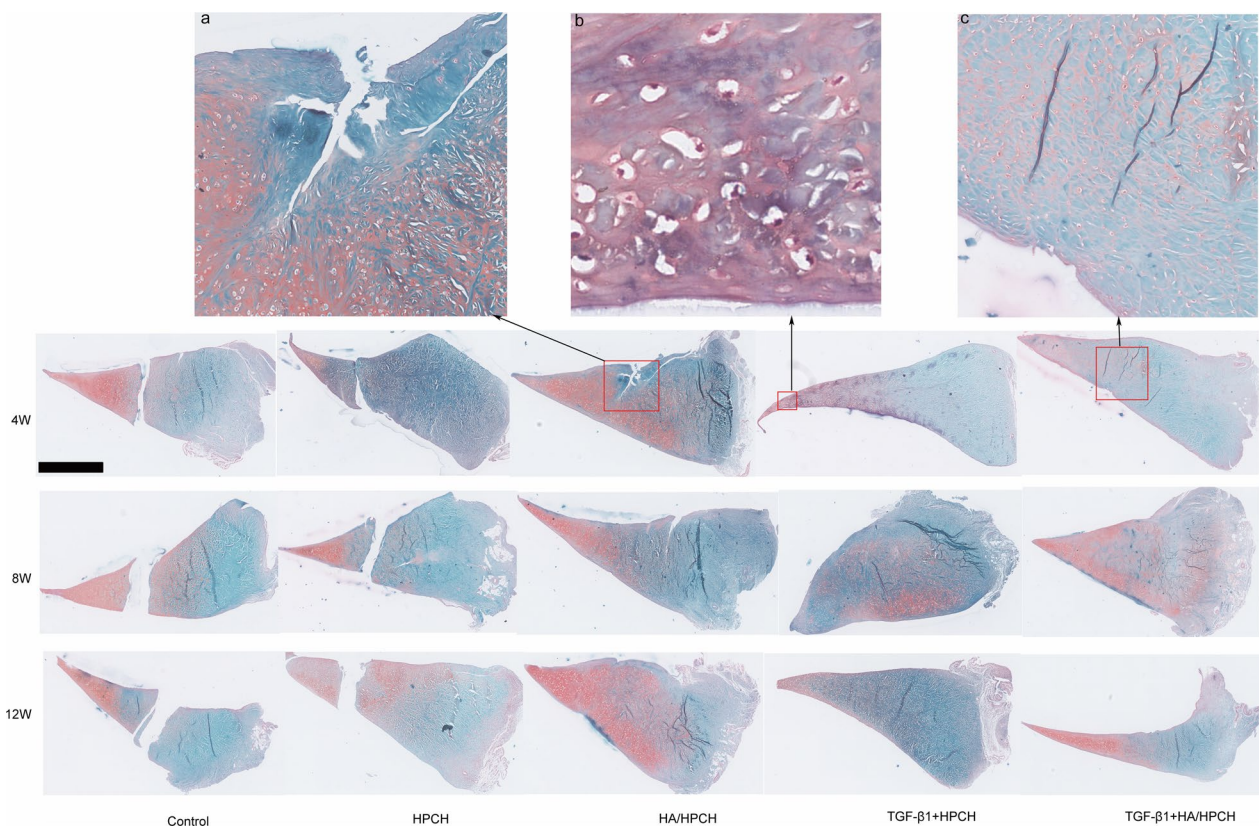


**Fig. 15** Safranin-O-fast green staining of menisci. Group A, HA/HPCH; group B, TGF- $\beta$ 1 + HPCH; group C, TGF- $\beta$ 1 + HA/HPCH; Scale bar, 1 mm

response was seen in the knee joint at 12 weeks; while TGF- $\beta$ 1 + HPCH and HA/HPCH hydrogels could promote the repair of meniscus injury, but the effect was slightly poorer than that of TGF- $\beta$ 1 + HA/HPCH hydrogel. The menisci of nine rabbits in the control group and HPCH group did not heal; however, those of six, six, and seven rabbits in the TGF- $\beta$ 1 + HPCH, HA/HPCH, and TGF $\beta$ 1 + HA/HPCH groups, respectively, did exhibit healing. We speculate that MFCs are not simply an inert cell in the body. TGF- $\beta$ 1 and HA can strengthen the migration and adhesion of MFCs and stimulate the secretion of GAG, sugar and other ECM components, while the inside of the gel can provide a good three-dimensional microenvironment to promote cell growth and proliferation. With the growth of cells, the scaffold material slowly degrades and is gradually replaced by ECM secreted by cells. With the increase of ECM, the damaged area of the meniscus is gradually and completely repaired.

In this process, it is not possible to determine whether the cells in the hydrogel migrated from normal meniscus or synovial tissue, or whether both are involved in the repair process. To prove these speculations, strict *in vivo* cell tracking methods should be conducted in future studies. In animal models, there are no clear pain and

functional evaluation standards. Thus, we cannot determine whether the rabbit knee joint is painful, whether its function is good, and whether there is dysfunction compared with the normal knee joint. In this study, the follow-up period was limited due to time constraints. The future studies should include a longer follow-up duration to fully assess the long-term outcomes of this treatment approach, such as 6 months or 1 year. At present, the specific mechanism by which HA promotes meniscus injury repair remains unclear. In subsequent studies, the specific cellular pathways involved in HA promotion of meniscus cell migration, growth, and proliferation should be further explored, along with the specific cellular pathways that promote the secretion of ECM by MFCs. We hope that the next step is to apply these findings in a clinical setting and conduct on clinical trials of human patients to confirm the safety and effectiveness of this treatment in real-world clinical practice.

We believe that, for meniscus injury, providing an appropriate scaffold material and adding growth factors or seed cells or even more factors to participate together can promote the differentiation, growth, and proliferation of cells derived from MFCs or synovial tissue to secrete and synthesize ECM, and ultimately achieve repair of

meniscus white area damage. In this study, we added HA and TGF- $\beta$ 1, both of which have an effect on the repair of meniscus damage. Considering the price and storage conditions, HA may have a broader application prospect in the repair of meniscus damage.

## Conclusions

In this study, we proved that the HPCH hydrogel loaded with HA and TGF- $\beta$ 1 provides a suitable environment to enhance the repair potential of meniscus injury. The hybrid scaffold with HA and TGF- $\beta$ 1 shows excellent meniscus injury repairing ability. The addition of HA alone also has the potential to strengthen the repair of meniscus damage. Although this experiment does have some limitations, loading may be a promising strategy for the repair of meniscus damage in the future. In clinical applications, we can fill the gap after meniscus suture with TGF- $\beta$ 1+HA/HPCH hydrogel to enhance the regeneration ability of the damaged meniscus, meaning the repaired tissue and the physical function and biological characteristics of the normal meniscus are consistent.

## Abbreviations

TGF- $\beta$ 1	Transforming growth factor $\beta$ 1
GAG	Glycosaminoglycan
HPCH	Hydroxypropyl chitin
HA	Hyaluronic acid
MFCs	Meniscal fibrochondrocytes
ECM	Extracellular matrix
BMP-2	Bone morphogenetic protein 2
IGF-1	Insulin-like growth factor 1
CCK-8	Cell counting kit 8

## Author contributions

ZW WH SJ FG TS YH XJ HW ZW WH and SJ carried out the concepts, design, definition of intellectual content, literature search, data acquisition, and manuscript preparation. FG, TS, YH carried out literature search, data acquisition and manuscript editing. XJ and HW devised the project, the main conceptual ideas and performed manuscript review.

## Funding

National Natural Science Foundation of China, Grant/Award Number: 81672166.

## Availability of data and materials

No datasets were generated or analysed during the current study.

## Declarations

## Competing interests

The authors declare no competing interests.

Received: 30 July 2024 Accepted: 4 October 2024

Published online: 23 October 2024

## References

- George J, Kazunori S, Krych AJ, et al. The meniscus tear: a review of stem cell therapies. *Cells*. 2019;9(1):92.

- Hulet C, Menetrey J, Beaufils P, et al. Clinical and radiographic results of arthroscopic partial lateral meniscectomies in stable knees with a minimum follow up of 20 years. *Knee Surg Sports Traumatol Arthrosc*. 2015;23(1):225–31.
- Kopf S, Beaufils P, Hirschmann MT, et al. Management of traumatic meniscus tears: the 2019 ESSKA meniscus consensus. *Knee Surg Sports Traumatol Arthrosc*. 2020;28(4):1177–94.
- Seil R, Becker R. Time for a paradigm change in meniscal repair: save the meniscus! *Knee Surg Sports Traumatol Arthrosc*. 2016;24(5):1421–3.
- Bilgen B, Jayasuriya CT, Owens BD. Current concepts in meniscus tissue engineering and repair. *Adv Healthc Mater*. 2018;7(11):e1701407.
- Rey-Rico A, Cucchiari M, Madry H. Hydrogels for precision meniscus tissue engineering: a comprehensive review. *Connect Tissue Res*. 2017;58(3–4):317–28.
- Zhang Z, Guo W, Gao S, et al. Native tissue-based strategies for meniscus repair and regeneration. *Cell Tissue Res*. 2018;373(2):337–50.
- Panyamao P, Ruksiriwanich W, Sirisa-Ard P, Charumanee S. Injectable thermosensitive chitosan/pullulan-based hydrogels with improved mechanical properties and swelling capacity. *Polymers (Basel)*. 2020;12(11):2514.
- Guo W, Xu W, Wang Z, et al. Cell-free strategies for repair and regeneration of meniscus injuries through the recruitment of endogenous stem/progenitor cells. *Stem Cells Int*. 2018;12(2018):5310471.
- Kwon H, Brown WE, Lee CA, et al. Surgical and tissue engineering strategies for articular cartilage and meniscus repair. *Nat Rev Rheumatol*. 2019;15(9):550–70.
- Deng X, Chen X, Geng F, et al. Precision 3D printed meniscus scaffolds to facilitate hMSCs proliferation and chondrogenic differentiation for tissue regeneration. *J Nanobiotechnology*. 2021;19(1):400.
- Zhou ZX, Chen YR, Zhang JY, et al. Facile strategy on hydrophilic modification of poly( $\epsilon$ -caprolactone) scaffolds for assisting tissue-engineered meniscus constructs in vitro. *Front Pharmacol*. 2020;11(11):471.
- Resmi R, Parvathy J, John A, et al. Injectable self-crosslinking hydrogels for meniscal repair: a study with oxidized alginate and gelatin. *Carbohydr Polym*. 2020;15(234):115902.
- Ghodbane SA, Brzezinski A, Patel JM, et al. Partial meniscus replacement with a collagen-hyaluronan infused three-dimensional printed polymeric scaffold. *Tissue Eng Part A*. 2019;25(5–6):379–89.
- Baek J, Sovani S, Glembotski NE, et al. Repair of avascular meniscus tears with electrospun collagen scaffolds seeded with human cells. *Tissue Eng Part A*. 2016;22(5–6):436–48.
- Ying XZ, Qian JJ, Peng L, et al. Model research on repairing meniscus injury in rabbits using bone marrow mesenchymal stem cells and silk fibroin meniscus porous scaffold. *Eur Rev Med Pharmacol Sci*. 2018;22(12):3689–93.
- Gunes OC, Kara A, Baysan G, et al. Fabrication of 3D printed poly(lactic acid) strut and wet-electrospun cellulose nano fiber reinforced chitosan-collagen hydrogel composite scaffolds for meniscus tissue engineering. *J Biomater Appl*. 2022;37(4):683–97.
- Yu Z, Lili J, Tiezheng Z, et al. Development of decellularized meniscus extracellular matrix and gelatin/chitosan scaffolds for meniscus tissue engineering. *Biomed Mater Eng*. 2019;30(2):125–32.
- Pillai MM, Gopinathan J, Selvakumar R, et al. Human knee meniscus regeneration strategies: a review on recent advances. *Curr Osteoporos Rep*. 2018;16(3):224–35.
- Abpeikar Z, Javdani M, Mirzaei SA, et al. Macroporous scaffold surface modified with biological macromolecules and piroxicam-loaded gelatin nanofibers toward meniscus cartilage repair. *Int J Biol Macromol*. 2021;31(183):1327–45.
- Abpeikar Z, Moradi L, Javdani M, et al. Characterization of macroporous polycaprolactone/silk fibroin/gelatin/ascorbic acid composite scaffolds and in vivo results in a rabbit model for meniscus cartilage repair. *Cartilage*. 2021;13(2\_suppl):1583S–1601S.
- Li Z, Wu N, Cheng J, et al. Biomechanically, structurally and functionally meticulously tailored polycaprolactone/silk fibroin scaffold for meniscus regeneration. *Theranostics*. 2020;10(11):5090–106.
- Yuan M, Bi B, Huang J, et al. Thermosensitive and photocrosslinkable hydroxypropyl chitin-based hydrogels for biomedical applications. *Carbohydr Polym*. 2018;15(192):10–8.
- Bayer IS. Hyaluronic acid and controlled release: a review. *Molecules*. 2020;25(11):2649.

25. Gupta RC, Lall R, Srivastava A, et al. Hyaluronic acid: molecular mechanisms and therapeutic trajectory. *Front Vet Sci*. 2019;25(6):192.
26. Delaney K, Kasprzycka P, Ciemerych MA, et al. The role of TGF- $\beta$ 1 during skeletal muscle regeneration. *Cell Biol Int*. 2017;41(7):706–15.
27. Xia P, Wang S, Qi Z, et al. BMP-2-releasing gelatin microspheres/PLGA scaffolds for bone repairment of X-ray-radiated rabbit radius defects. *Artif Cells Nanomed Biotechnol*. 2019;47(1):1662–73.
28. Fortier LA, Barker JU, Strauss EJ, et al. The role of growth factors in cartilage repair. *Clin Orthop Relat Res*. 2011;469(10):2706–15.
29. Chen M, Guo W, Gao S, et al. Biochemical stimulus-based strategies for meniscus tissue engineering and regeneration. *Biomed Res Int*. 2018;17(2018):8472309.
30. MacBarb RF, Makris EA, Hu JC, et al. A chondroitinase-ABC and TGF- $\beta$ 1 treatment regimen for enhancing the mechanical properties of tissue-engineered fibrocartilage. *Acta Biomater*. 2013;9(1):4626–34.
31. Wang X, Wang Y, Yan M, et al. Thermosensitive hydrogel based on poly(2-ethyl-2-oxazoline)-poly(D, L-lactide)-poly(2-ethyl-2-oxazoline) for sustained salmon calcitonin delivery. *AAPS PharmSciTech*. 2020;21(2):71.
32. Zhang K, Xue K, Loh XJ. Thermo-responsive hydrogels: from recent progress to biomedical applications. *Gels*. 2021;7(3):77.
33. Sionkowska A, Gadomska M, Musiał K, et al. Hyaluronic acid as a component of natural polymer blends for biomedical applications: a review. *Molecules*. 2020;25(18):4035.
34. Ladiè R, Cosentino C, Tagliaro I, et al. Supramolecular structuring of hyaluronan–lactose-modified chitosan matrix: towards high-performance biopolymers with excellent biodegradation. *Biomolecules*. 2021;11(3):389.
35. Ragland SA, Criss AK. From bacterial killing to immune modulation: recent insights into the functions of lysozyme. *PLoS Pathog*. 2017;13(9):e1006512.
36. Ghazi Zadeh L, Chevrier A, Farr J, et al. Augmentation techniques for meniscus repair. *J Knee Surg*. 2018;31(1):99–116.
37. Pangborn CA, Athanasiou KA. Effects of growth factors on meniscal fibrochondrocytes. *Tissue Eng*. 2005;11(7–8):1141–8.
38. de Mulder EL, Hannink G, Giele M, et al. Proliferation of meniscal fibrochondrocytes cultured on a new polyurethane scaffold is stimulated by TGF- $\beta$ . *J Biomater Appl*. 2013;27(5):617–26.
39. Hagmeijer MH, Korpershoek JV, Crispim JF, et al. The regenerative effect of different growth factors and platelet lysate on meniscus cells and mesenchymal stromal cells and proof of concept with a functionalized meniscus implant. *J Tissue Eng Regen Med*. 2021;15(7):648–59.
40. Du X, Liu Y, Wang X, et al. Injectable hydrogel composed of hydrophobically modified chitosan/oxidized-dextran for wound healing. *Mater Sci Eng C Mater Biol Appl*. 2019;104:109930.
41. Norouzi M, Nazari B, Miller DW. Injectable hydrogel-based drug delivery systems for local cancer therapy. *Drug Discov Today*. 2016;21(11):1835–49.
42. Murakami T, Otsuki S, Okamoto Y, et al. Hyaluronic acid promotes proliferation and migration of human meniscus cells via a CD44-dependent mechanism. *Connect Tissue Res*. 2019;60(2):117–27.
43. Viganì B, Rossi S, Sandri G, et al. Hyaluronic acid and chitosan-based nanosystems: a new dressing generation for wound care. *Expert Opin Drug Deliv*. 2019;16(7):715–40.
44. Tan H, Chu CR, Payne KA, Marra KG. Injectable in situ forming biodegradable chitosan-hyaluronic acid based hydrogels for cartilage tissue engineering. *Biomaterials*. 2009;30(13):2499–506.

## Publisher's Note

Springer Nature remains neutral with regard to jurisdictional claims in published maps and institutional affiliations.